SANTA LAURENSIA
Alam Sutera

Design and Optimization of Solar-Powered Glove Warmer

Yutaka Taro Kusumah

Callie Sebastianus

SMA Santa Laurensia Alam Sutera

Tangerang, Banten

2024

ABSTRACT

This research aimed to develop and evaluate a sustainable heated glove powered by solar energy, designed for use in environments where conventional electricity is limited. The glove utilizes carbon fiber heating elements, integrated with a rechargeable 3.7 V Li-Po battery and a TP4056 solar charging circuit. The study investigated four heating configurations: dorsal-only, finger-only, combined dorsal and finger, and a control with no heating. Two researchers volunteered as test subjects, and trials were conducted under controlled ambient conditions. Skin temperature at the dorsal and middle finger regions was measured every two minutes over 20 minutes using a contactless infrared thermometer.

Data were modeled using nonlinear exponential regression to represent the gradual rise of skin temperature. Among all configurations, dorsal-only heating produced the highest rate of temperature increase, contradicting the initial hypothesis that finger heating would be most effective. The combined configuration showed a negative interaction effect, likely caused by increased circuit resistance reducing power delivery. The no-heating condition produced negligible change. All model coefficients were statistically significant ($p < 0.05$), and residual diagnostics supported the model's validity.

The findings confirm that solar-powered heating gloves are both feasible and effective, with dorsal heating providing the optimal thermal response. However, long-term temperature projections beyond 20 minutes remain uncertain due to data extrapolation. The glove design proved safe, functional, and portable, highlighting its potential for off-grid applications in cold environments.

Keywords: heated glove, carbon fiber, solar-powered device, nonlinear regression

CHAPTER 1. INTRODUCTION

1.1 BACKGROUND

Hands are particularly vulnerable to heat loss due to their frequent exposure to harsh weather conditions. In cold environments, the body's response prioritizes maintaining core temperature by redirecting blood flow away from extremities, significantly reducing circulation to the fingers. While this mechanism is essential for survival, it results in cold hands, often causing discomfort and impairing dexterity. Such effects can negatively impact mental focus, productivity, and overall well-being. For individuals exposed to extreme climates, such as outdoor workers or hikers, prolonged cold exposure exacerbates these challenges, leading to serious health risks, including frostbite, reduced grip strength, and increased susceptibility to injuries. These risks underscore the need for hand warmers, to address the impact of cold environments. (Burke, 2024)

Traditional hand warmers and gloves, despite their widespread use, fail to address key issues of environmental sustainability, practicality, and effectiveness. Disposable chemical hand warmers, which generate heat through iron oxidation, are single-use products (Wang, 2010) that contribute to environmental pollution through its disposal, containing raw compounds such as iron powder that can leak into the ground (Earth Reminder, 2023). Their design limits usability by requiring users to hold them, restricting hand functionality (Burke, 2024). While traditional gloves are generally considered sustainable and practical, they fail to provide sufficient warmth in extreme conditions as they rely solely on insulation. The reduced protection can put users at a discomfort or a health risk in extremely cold climates (Arcfomor, 2024).

Battery-heated gloves provide a significant improvement over traditional gloves and disposable hand warmers. Equipped with electrical heating elements, they provide adjustable warmth that exceeds the capabilities of chemical hand warmers and traditional gloves. Additionally, it has a rechargeable battery lasting 8 to 10 hours under normal conditions, contributing to greater environmental sustainability. However, battery-heated gloves still have drawbacks, mainly bulk, weight, cost, and practicality. The heating element reduces finger dexterity compared to traditional gloves of similar thickness. They are generally more expensive than traditional gloves, given their advanced technology and electrical systems. Moreover, the limited battery life necessitates carrying spare batteries, which increases weight during multi-day expeditions without access to power (Short Guys Beta Works, 2023; Arcfomor, 2024).

This research aims to address the practicality limitations of battery-heated gloves by integrating solar panels into their design. This eliminates the need for spare batteries, reducing both weight and additional costs. This research focuses on optimizing power consumption to improve energy efficiency. Although bulk and cost are acknowledged limitations, they fall outside the scope of this study. Through a comprehensive literature review, the best materials and designs will be identified. The methodology includes optimizing power consumption for the prototype, followed by the creation and testing of the finished product.

1.2 PROBLEM STATEMENT

1) Cold hands caused by cold environments result in discomfort and health risks, particularly for individuals exposed to extreme climates.
2) Traditional hand warmers and gloves fail to fully address the challenges of environmental sustainability, practicality, and effectiveness.
3) Existing battery-heated gloves provide a significant improvement but are hindered by bulk, weight, cost, and practicality.

1.3 RESEARCH QUESTIONS

1) How can solar panels be integrated into battery-heated gloves to ensure reliable functionality?
2) What configurations optimize power consumption for solar-powered glove warmers?

1.4 OBJECTIVES

1) To develop solar-powered glove warmers that provide sufficient power.
2) To evaluate the heating elements configurations that optimize power consumption in solar-powered glove warmers.

1.5 RESEARCH BOUNDARIES

The scope of this study will focus on the development of solar-powered glove warmers and the optimization of power consumption. Materials and designs are determined with literature review. Cost and bulk are acknowledged but not addressed in this research.

1.6 RESEARCH BENEFITS

1) Solar-powered gloves offer effective heating for cold hands, even in extreme climates, while being environmentally sustainable and practical to use.
2) Unlike traditional battery-heated gloves, solar-powered gloves eliminate the need for spare batteries, ensuring continuous functionality even in remote locations.

CHAPTER 2. LITERATURE REVIEW

2.1 OVERVIEW OF HEAT LOSS IN HANDS AND ITS IMPACTS

Hands are particularly vulnerable to heat lost due to their anatomical structure. It has a large surface area to volume ratio which is 4 to 5 times larger than the body and causes rapid heat loss (Zhang, 2021). At temperatures lower than 15.0 °C, finger dexterity and sensitivity begin to reduce, which is a great hazard towards occupational health and safety; this is caused by its association towards obstructing the worker's accuracy and efficiency. This is especially challenging for workers who work in extremely cold conditions, such as polar peaks or ocean depths, and may be exposed to extreme climates that result in numbness or frostbite (Ma et al., 2018).

2.2 DESIGN OF ELECTRICALLY HEATING GLOVES

According to Nini Ma et al., the electrically heating gloves (EHG) system is composed of gloves, heating elements, and a temperature control mode (Ma et al., 2018). Temperature control modes are beyond the purpose of this research and will not be reviewed.

2.2.1 GLOVES

The glove is made of an inner layer, and the shell, which is subdivided into a three-layer composite system, being the outer layer, moisture barrier, and thermal liner. In our experiment, we will follow the materials of EHG being used for the experiments by Nini Ma et al. except the thermal liner, discussed below, being (Ma et al., 2018):

Table 1: *Glove Material Composition*

Structure	Component	Materials
Shell Layer	Outer Layer	100% Polyester
	Moisture Barrier	PTFE Film
	Thermal Liner	PE Foam Cotton (Closed-Cell Type)
Inner Layer	Inner Layer	100% Nylon

EPE foam cotton is replaced by PE foam cotton for the thermal liner, due to the following reasons. The cost of PE foam cotton is much lower than EPE foam cotton. Comparing their performance, PE Foam has a higher temperature resistance, stronger, more durable, and provides better electrical and thermal insulation than EPE foam cotton, while both being waterproof. Lastly, PE foam is more environmentally friendly to manufacture, and can be entirely recycled and reused for new applications (Foam Industries, n.d.).

2.2.2 FLEXIBLE HEATING ELEMENT

The heating element and its connector was put between the thermal liner and inner layer and fixed to the back side of the gloves, as the back required more temperature protection. Flexible heating element is composed of conductive material and substrate material. The conductive material can be metallic, such as metal fiber, metal nanowires, etc., and nonmetallic, including carbon fibers, conductive polymers, and carbon nanomaterials. The type of substrate material determines the

flexibility, stability, and safety, and mainly categorized into flexible heating fabric, flexible heating film, and multi-functional flexible heating elements.

Multi-functional flexible heating elements include supplementary functions on top of the heating elements, including heat sensors, thermochromic materials (changes color with temperature change), that are irrelevant to the purpose of this research. Flexible heating film requires hardly accessible and expensive materials, such as conductive polymers, electrothermal film, or multi-walled carbon nanotubes that are beyond the scope of this research. Hence, this research will focus on flexible heating fabric. Below are the summary of materials and preparation of heating fabrics:

Table 2: *Potential Materials for Heating Fabrics*

Conductive Materials	Substrate Materials	Preparation Method	Load Voltage (V)	Maximum Equilibrium Temperature (°C)	Resistivity/ Conductivity
Metal based					
Stainless steel yarns	Polyester knitting fabric	Weaving	12	60	–
AgNWs	Cotton fabric	Impregnation	6	150	2.5 Ωsq^{-1}
CuNWs	PE fibers	Dipping	3	57	–
Silver- plated yarn	Polyester staple yarn	Knitting	4	70	–
Polymer based					
Polypyrrole	Nylon fabric	Chemical and electrochemical coating	3.6	55	5 Ωsq^{-1}
Polypyrrole	Cotton fabric	In situ polymerization	9	83	303 Ωsq^{-1}
Polyethylene dioxophene thiophene	PET	Vapor phase polymerization	15	43	52 Ωsq^{-1}
Carbon based					
Recycled carbon fiber	Non-woven fabric	Wet paper process	13	94.6	2.8×10^{3} Sm^{-1}
SWCNTs	Cotton fabric	Dipping and coating	40	96	5 kΩ
Reduction graphene	Polyester	Vapor deposition	6	50	24.7 Ωsq^{-1}

oxide

Graphene	Cotton woven fabric	Spraying	12	162.6	–
Graphene/ waterborne polyurethane	Para aramid knitted fabric	Impregnation and hot pressing	50	58.4	7.5×10^4 Ωsq^{-1}

Subsequent researches ruled out heating fabrics made using hardly accessible or expensive, or manufactured using specialized and complex equipment, leaving only the sole production method that is easily manufactured or purchased, being carbon fibers (Fang et al., 2020).

As recycled carbon fiber is a three-dimensional structure, its resistivity can be measured using Ωm. The graph measured the conductivity of recycled carbon fiber as 2.8×10^3 Sm^{-1}, where Sm^{-1} is siemen metre^{-1}, the SI unit of conductivity. The reciprocal of electrical conductivity, denoted by σ, is the reciprocal of resistivity, denoted by ρ. Hence, the following formula can be used:

$$\sigma = \frac{1}{\rho}$$

Then, the resistivity of recycled carbon fiber can be calculated as:

$$\rho = \frac{1}{\sigma} \Rightarrow \frac{1}{2.8 \times 10^3\ Sm^{-1}} = 3.57 \times 10^{-4}\ \Omega m$$

Resistance can be calculated with the following formula:

$$R = \rho \frac{l}{A}$$

Where

ρ is the electrical resistivity of the material

l is the specimen length

A is the cross-sectional area of the specimen.

Note that carbon is a semiconductor, and the resistivities of semiconductors are more than those of conductors, being around 10x - 10000x higher than pure metals or alloys (Kumar, 2004, pp. 282-284).

2.2.2.1 RESISTIVE HEATING

When electrical current passes through a material with a resistance, some of the energy will be dissipated as heat. This heat is measured in terms of power, which is the rate at which energy is being converted into heat.

The formulas to calculate the amount of heat dissipated in a resistor are

$$P = I^2 R$$

Where P is the power, I is the current, and R is the resistance (Meier, 2006, pp. 14-16).

2.3 HEATING ELEMENTS PLACEMENTS

According to Kempson et al., the electrical heating elements in the gloves can be arranged to heat the entire hand or simply only the fingers. Initial studies indicate the biggest efficiency and cost effectiveness of electric power occurs when only the fingers alone are warmed, as opposed to heating the palm or the back of the hand. This shows that the most beneficial effect can be achieved from heating the fingers, such that focusing on the fingers will prolong the heating time that the battery packs support without recharging (Kempson et al., 2007, p. 1088).

2.4 SOLAR PANEL MATERIALS

Solar panels mainly use two forms of silicon to convert light to electricity, being polycrystalline or monocrystalline silicon. Monocrystalline silicon ingots are sliced and polished into 1 mm or 0.0393 inches silicon wafers. The wafer's edges then got etched and roughened to improve their efficiency and prevent light reflection as much as possible. The structure of the wafers allows it to have higher efficiency rates usually between 15% - 23%. However, they have high initial costs since their manufacturing process is energy intensive and produces large amounts of silicone waste (American Solar Energy Society, 2021). Most monocrystalline solar panels have a power output of 160 watts per m^2. They also have a temperature coefficient of around -0.3 %/°C to -0.4 %/°C which will decrease in output for every 1°C increase in temperature over 25°C (Ryan, n.d.).

2.5 HYPOTHESIS

1) There is a significant difference in skin heating rates between normal and powered gloves.
2) Among all tested configurations, heating elements placed on the finger region result in the highest rate of skin heating.

CHAPTER 3. METHODOLOGY

3.1 TIME AND PLACE OF RESEARCH

Start date : March 2025, SMA Santa Laurensia Alam Sutera Lab Physics 2

Table 3: *Research Timeline*

Procedure	Dates
Materials Collection	4 – 11 March
Experimental Trials	11 March – 20 May
Data Analysis & Conclusion	20 – 25 May

3.2 VARIABLES

The independent variable in this study is the placement of the heating elements on the glove, with four configurations tested: (i) dorsal region of the hand, (ii) back of the finger, (iii) both dorsal and finger regions, and (iv) no heating (control). The dependent variable is the skin surface temperature of the hand, measured at two locations: the back of the hand (dorsal) and the back of the middle finger. Control variables include the initial skin temperature (36.0 °C), ambient conditions, clothing worn, seated posture, and absence of physical activity or heat-altering substances before testing.

3.3 TOOLS AND MATERIALS

- Gloves: Constructed using 100% polyester fabric, closed-cell polyethylene (PE) foam cotton (thermal liner), and 100% nylon fabric.
- Heating Elements: Carbon fiber and polymer composite, used as a substitute for recycled carbon fiber embedded in a non-woven fabric composite.
- Electrical Components: Solar panels, a rechargeable 3.7 V lithium-polymer (Li-Po) 2000 mAh battery, and various supporting components including resistors, a 50 °C thermostat, wiring, switch, and fuse.
- Sensors: Contactless infrared thermometer for skin temperature measurements and multimeter and digital multimeter for measuring voltage, current, and resistance in the electrical circuit.

3.4 RESEARCH DESIGN AND PROCEDURE

This study employed a repeated-measures experimental design, in which two volunteer researchers (one male and one female) served as test subjects and underwent all four glove configurations. The data collected were quantitative time-series measurements of skin temperature.

To reduce confounding variables, both participants were instructed to abstain from consuming food, alcohol, or engaging in physical activity for 24 hours prior to testing. All trials were conducted under consistent ambient conditions, with subjects wearing standardized casual clothing and receiving no prior cold exposure.

The solar-powered heated gloves were constructed before testing, using carbon fiber heating elements and a solar-rechargeable electrical circuit. The experiment involved four configurations: (i) heating at the back of the finger, (ii) heating at the dorsal region of the hand, (iii) heating at both zones, and (iv) a control with no heating.

Before each trial, participants cooled their hands to an equilibrium skin temperature of approximately 36.0 °C. During the trial, they maintained a half-clenched posture with the gloved

hand resting on a table. Skin temperature was recorded using a contactless infrared thermometer at two anatomical sites: the dorsal hand and the back of the middle finger. Readings were taken every 2 minutes over a 20-minute period (11 total time points). Data were recorded using structured observation sheets for temperature to ensure consistent logging. A visual flowchart illustrating the full research procedure is provided in Figure 1.

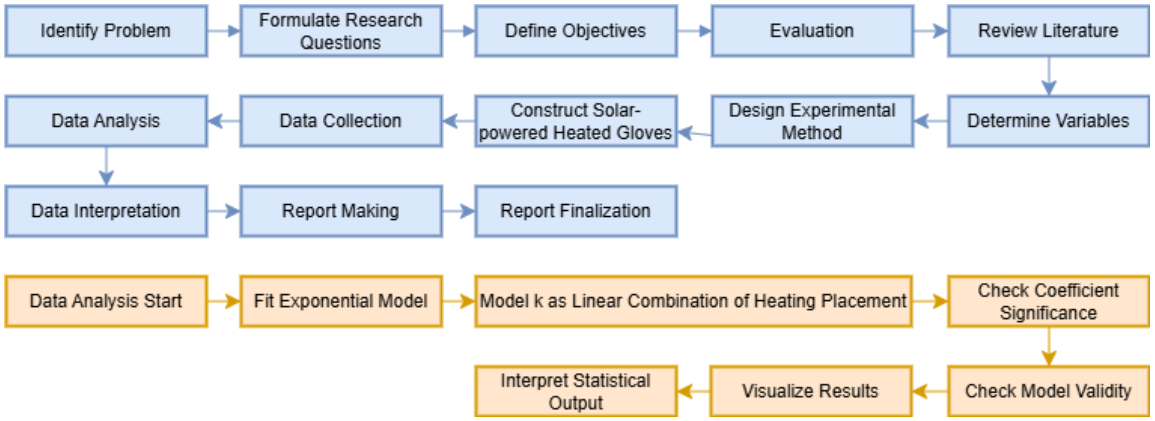

Figure 1: *Research Plan Flowchart*

3.5 DATA PROCESSING AND ANALYSIS

Temperature data were modeled using nonlinear exponential regression, as skin temperature is expected to increase rapidly during initial heating and then gradually approach an equilibrium. The model used to represent this behavior was:

$$T(t) = T_0 + A \times (1 - e^{-kt})$$

Where

- $T(t)$ – Skin temperature at time t,
- T_0 – Initial skin temperature,
- A – Amplitude, maximum skin temperature increase from the baseline,
- k – Rate constant; a higher k value indicates a faster rate of heating.

To determine whether the rate of heating was significantly influenced by heating placement, the rate constant k was expressed as a linear combination of binary variables indicating the presence of dorsal and/or finger heating:

$$k = \beta_0 + \beta_1 \cdot dorsal + \beta_2 \cdot finger + \beta_3 \cdot (dorsal \times finger)$$

To effectively compare heating rates across configurations, the fitted temperature–time model will be evaluated at t = 5, 20, and 60 minutes, representing short-term, medium-term, and long-term heating intervals, respectively.

Model fitting and statistical significance (via p-values of the regression coefficients) were evaluated using the lmfit package in Python. A significance threshold of $p < 0.05$ was used. Standard deviation was not reported, as no repeated trials were taken. R-squared and adjusted R-squared values were not calculated, as they assume a linear model structure. This assumption does not hold for the exponential model used in this study, which is inherently nonlinear.

CHAPTER 4. DATA AND ANALYSIS

4.1 RAW DATA

Table 4: *Skin Temperature (Dorsal Area) under Varying Heating Configurations*

Time since heating (min)	Repetition 1, Heating Placements				Repetition 2, Heating Placements			
	Dorsal	Finger	Both	None (Control)	Dorsal	Finger	Both	None (Control)
	°C	*°C*	*°C*	*°C*	*°C*	*°C*	*°C*	*°C*
0	36.2	36.3	36.3	36.3	36.2	36.1	36.2	36.0
2	37.5	36.8	37.2	36.3	36.8	36.3	36.6	35.9
4	38.0	36.7	37.4	36.3	36.8	36.5	36.7	35.9
6	39.6	36.9	38.3	36.3	37.8	36.4	37.1	36.0
8	38.3	37.0	37.7	36.3	38.2	36.3	37.3	36.1
10	39.1	36.9	38.0	35.8	37.9	36.5	37.2	36.1
12	39.7	37.0	38.4	35.8	38.1	36.8	37.5	36.2
14	40.6	36.9	38.8	35.8	38.4	36.6	37.5	36.2
16	39.8	36.8	38.3	35.6	38.2	36.3	37.3	36.4
18	40.6	36.8	38.7	35.6	39.5	37.1	38.3	36.4
20	39.9	37.3	38.6	35.6	40.1	37.5	38.8	36.3

Table 5: *Skin Temperature (Middle Finger, Back) under Varying Heating Configurations*

	Repetition 1, Heating Placements	Repetition 2, Heating Placements

since heating (min)	Dorsal °C	Finger °C	Both °C	None (Control) °C	Dorsal °C	Finger °C	Both °C	None (Control) °C
0	35.9	36.2	36.1	35.5	36.2	35.9	36.1	36.3
2	36.7	37.2	37.0	35.5	36.6	36.8	36.7	36.4
4	36.8	37.2	37.0	35.6	36.7	36.8	36.8	36.2
6	36.7	37.2	37.0	35.4	36.5	37.1	36.8	36.5
8	36.9	37.7	37.3	36.1	36.9	37.2	37.1	36.6
10	37.2	38.1	37.7	36.0	37.1	37.1	37.1	36.2
12	36.7	38.2	37.5	36.1	36.8	37.3	37.1	36.4
14	36.3	37.8	37.1	35.8	36.7	37.6	37.2	36.5
16	37.6	38.1	37.9	35.6	36.9	37.8	37.4	36.5
18	37.3	38.1	37.7	35.8	37.2	37.8	37.5	36.6
20	36.7	38.2	37.5	35.9	37.1	37.9	37.5	36.5

4.2 STATISTICAL ANALYSIS

Skin temperature was calculated by first averaging the values recorded at the dorsal area and the back of the middle finger. For repeated trials, the resulting values were then averaged across repetitions to obtain the final temperature profile used in the analysis.

Exponential regression was used to model skin temperature increase over time, with the rate constant k modeled as a function of heating placement. Table 6 summarizes the fitted parameters and their statistical significance.

Table 6: *Models Fit Summary*

Parameter	Estimate	Std Error	t-value	p-value	Rel Error (%)
B0	-0.00464	0.00184	-2.521	0.0117	39.66
B1	0.07036	0.00704	9.999	< 0.0001	10.00
B2	0.03388	0.00326	10.403	< 0.0001	9.61
B3	-0.05000	0.00660	-7.572	< 0.0001	13.21

Table 7 presents predicted temperature increases for three heating configurations at t = 5, 20, and 60 minutes, representing short-term, medium-term, and long-term heating intervals. The left panel shows the absolute temperature increase (ΔT in °C), while the right panel expresses this as a percentage relative to the Finger configuration, which is set as 100% at each time point.

Table 7: *Time-Temperature Model Prediction*

	Absolute ΔT (°C)			Absolute ΔT (% of Finger)		
	5 min	20 min	60 min	5 min	20 min	60 min
Finger	0.41	1.34	2.50	100.0	100.0	100.0
Both	0.67	1.90	2.87	161.5	142.1	114.8
Dorsal	0.85	2.21	2.96	206.0	165.2	118.6

4.3 DIAGRAM

Figure 2 displays the observed skin temperature data alongside the fitted exponential curves for each heating configuration. Figure 3 presents the predicted temperature increases (ΔT) at t = 5, 20, and 60 minutes, along with their relative values compared to the Finger configuration. Figure 4 provides a residuals analysis to assess the validity of model assumptions, including normality, homoscedasticity (constant variance), and model fit.

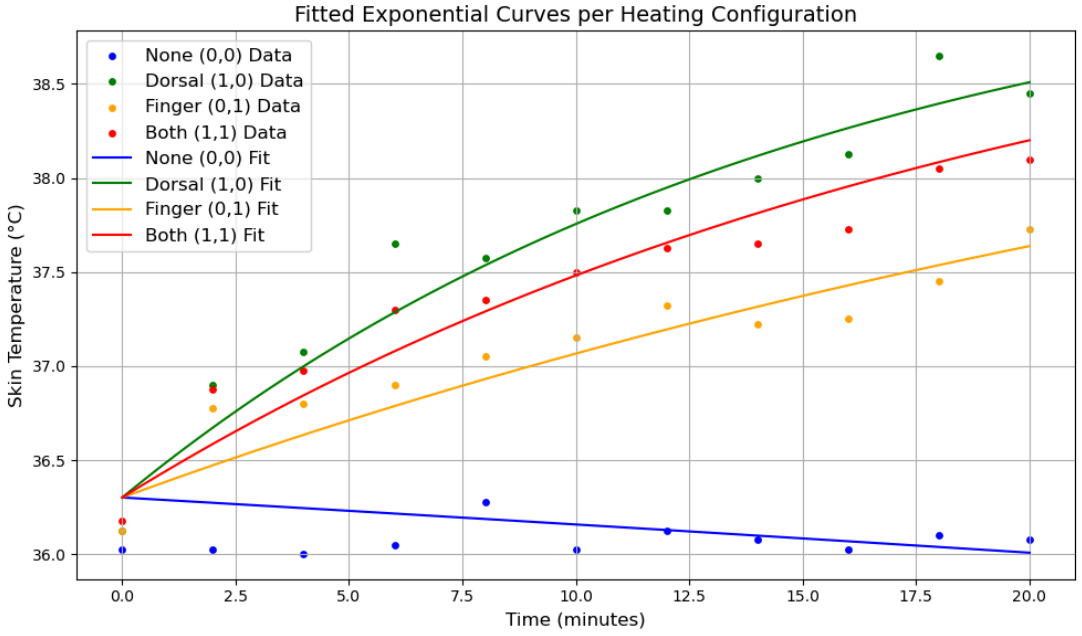

Figure 2: *Fitted Temperature Curves*

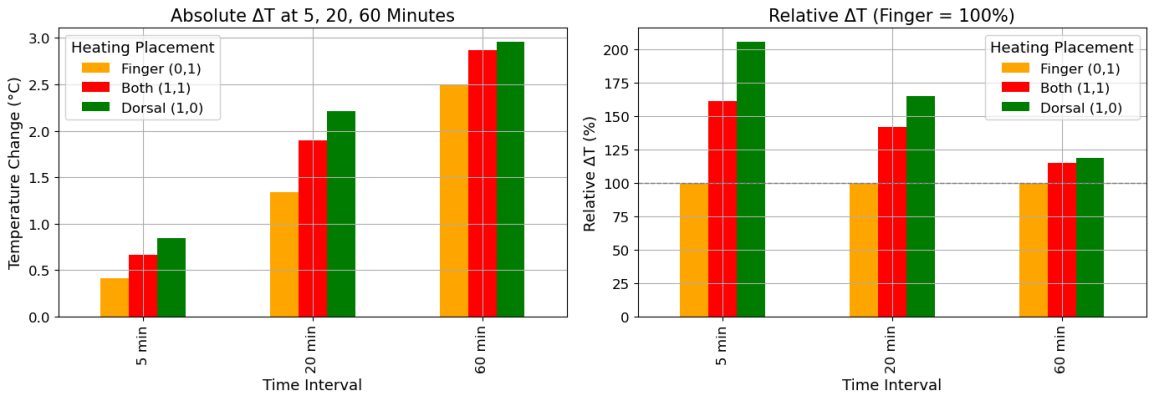

Figure 3: *Predicted Temperature Increase (ΔT) at 5, 20, and 60 Minutes*

The figure below shows a histogram of the residuals and the Q-Q plot of residuals quantiles against a theoretically perfect normally distributed quantiles to check normality, and fitted vs residuals plot to check whether error terms are uncorrelated and homoscedastic (constant variance).

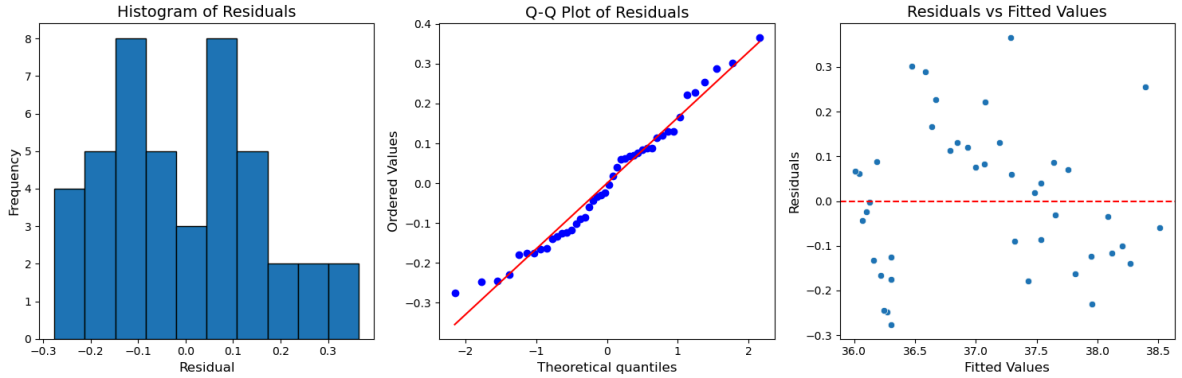

Figure 4: *Residuals Diagnostics for the Exponential Model Fit*

4.4 INTERPRETATION

The fitted exponential regression model reveals distinct differences in the effectiveness of each heating configuration. Dorsal-only heating consistently demonstrated the highest heating rate coefficient ($B_1 \approx 0.0704$) and a considerably higher temperature increase in different timespan (short-term, medium-term, long-term), making it the most effective configuration overall in increasing skin temperature. This indicates that targeting the dorsal side of the hand alone yields the fastest and most efficient thermal response.

In contrast, the combined dorsal + finger configuration performed worse than dorsal-only, despite incorporating both heating zones. This counterintuitive result is explained by the negative interaction coefficient ($B_3 \approx -0.0500$), which suggests that the combined configuration is counterproductive. One likely cause is electrical resistance: adding more heating zones increases the total circuit resistance, which in turn reduces the power delivered due to fixed battery voltage. As resistance increases, less current flows through the system, resulting in lower effective heating despite a larger coverage area.

Surprisingly, finger-only heating also underperformed relative to dorsal-only heating, with a smaller coefficient ($B_2 \approx 0.0339$). This finding contradicts the original second hypothesis, which predicted that heating the fingers alone would yield the highest skin temperature increase. The likely explanation is similar: the increased resistance in the finger heating configuration limits power output, thereby diminishing its heating performance despite targeting a thermally sensitive area.

Meanwhile, the no-heating (control) configuration produced a negligible coefficient ($B_0 \approx -0.0046$)—at least 7 times smaller than the active heating configurations. This suggests that passive insulation alone provides minimal benefit in raising skin temperature, and the negative value may reflect ambient cooling during the test.

All regression coefficients were statistically significant ($p < 0.05$), confirming that each factor meaningfully affects the rate of heating. Residual diagnostics (Figure 3) show approximate normality and symmetry, with no major skew, supporting the model's overall validity and suggesting low systematic bias. Some structured residual patterns hint at the potential benefit of more complex or biologically informed models.

Finally, while the model enables extrapolated predictions (i.e., for $t = 60$ min), it should be noted that no temperature plateau was observed during the 20-minute trials. Thus, long-term heating

projections should be interpreted cautiously, as they fall outside the measured timeframe and may not reflect real-world thermal regulation or user safety limits.

4.5 CIRCUIT DESIGN AND TROUBLESHOOTING

The final glove heating system employs a simplified yet functional circuit designed for both performance and safety. The primary components of the heating circuit include a 3.7 V LiPo battery, a resistive carbon fiber heating element, a manual switch, a resistor for current limiting, a normally closed 50 °C thermostat, and an inline fuse. This configuration enables direct, regulated heating while minimizing risks associated with overheating or electrical failure. The thermostat functions as a mechanical temperature cutoff, interrupting current flow if the internal glove temperature exceeds 50 °C. Although the heating element may reach this internal threshold, the skin temperature is expected to remain lower due to heat transfer delay and tissue insulation, ensuring user safety.

Charging functionality is separated from the main heating circuit to support the use of a dedicated solar panel that is too large to fit inside the glove. The external power source is connected to a TP4056 lithium battery charging module and a DC jack adapter. This allows the glove to be charged independently using renewable energy and avoids subjecting the TP4056 module to high discharge currents during active use.

This final design was achieved through multiple iterations and extensive troubleshooting. Early versions of the circuit incorporated a TP4056 module and an MT3608 boost converter directly within the heating loop, both of which failed due to overheating and insufficient current handling capacity. Other issues encountered included incorrect thermostat types (e.g., normally open instead of normally closed), swelling and leakage of LiPo batteries, transformer instability, inconsistent soldering and wiring connections, and inadequate current supply from AA batteries. Carbon fiber overheating was also observed in configurations without current limiting.

Ultimately, the final configuration eliminates unnecessary and failure-prone components while retaining essential safety features. The use of a fuse, resistor, mechanical thermostat, and external switch provides layered protection against thermal and electrical hazards. The inclusion of a solar-powered charging system with circuit isolation ensures energy autonomy without compromising safety.

CHAPTER 5. CONCLUSION

This research successfully developed a solar-chargeable, battery-powered heated glove using carbon fiber as the heating element. Among all tested configurations, dorsal heating alone produced the highest rate of skin temperature increase consistently, making it the most effective placement. Finger heating also increased temperature but was less effective, contradicting the second hypothesis, which predicted it would perform best. This outcome is likely due to increased circuit resistance reducing power delivery in the finger configuration. Notably, the combined dorsal and finger setup performed worse than dorsal-only, not due to diminishing returns, but rather a negative interaction effect—where additional heating elements increase circuit resistance, reducing overall power delivery. Meanwhile, the glove without heating elements contributed negligibly to warming, showing a significant temperature difference compared to gloves with active heating, proving the first hypothesis. The final design, which includes a fuse, resistor, 50 °C thermostat, 3.7V Li-Po battery, and a solar-powered TP4056 charging circuit, proved functional, portable, and safe, with the solar panel enabling continuous charging without interfering with heating performance, addressing the question of how to power wearable heating systems sustainably.

However, the study is limited by the small number of repetitions per condition, which restricts statistical power and prevents meaningful variability analysis. No temperature plateau was observed, indicating the need for better thermal regulation. Future work should explore automated control systems, model refinement using biological thermoregulation data, and expanded testing across multiple users and environmental conditions. Despite these limitations, the research confirms that sustainable, solar-powered heating gloves are feasible and useful, with clear potential for applications in cold environments, field work, or emergency response where electricity access is limited.

REFERENCES

American Solar Energy Society. (2021, February 20). *Monocrystalline vs Polycrystalline Solar Panels*. American Solar Energy Society. Retrieved February 4, 2025, from https://ases.org/monocrystalline-vs-polycrystalline-solar-panels/

Arcfomor. (2024, November 11). *Advantages and Disadvantages of Heated Gloves Over Traditional Warm Gloves*. Advantages and Disadvantages of Heated Gloves Over Traditional Warm Gloves. Retrieved January 17, 2025, from https://www.arcfomor.com/blogs/stay-warm-and-active-the-ultimate-guide-to-thin-heated-gloves/advantages-and-disadvantages-of-heated-gloves-over-traditional-warm-gloves

Burke, J. (2024, December 12). *How to Keep Your Hands Warm in Cold Weather*. How to Keep Your Hands Warm in Cold Weather. Retrieved January 16, 2025, from https://www.heatholders.com/blogs/wow/how-to-keep-your-hands-warm-in-cold-weather

Earth Reminder. (2023, September 14). *Are Hand Warmers Bad For The Environment?* Earth Reminder. Retrieved January 16, 2025, from https://www.earthreminder.com/are-hand-warmers-bad-for-the-environment/

Fang, S., Wang, R., Ni, H., Liu, H., & Liu, L. (2020, October 28). A review of flexible electric heating element and electric heating garments. *Journal of Industrial Textiles*, *51*(1), 101S-136S. https://doi.org/10.1177/1528083720968278

Foam Industries. (n.d.). *XLPE vs PE vs EPE Foam: Which One is Better?* XLPE vs PE vs EPE Foam: Which One is Better? Retrieved February 8, 2025, from https://www.foam-industries.com/news/xlpe-vs-pe-vs-epe-foam-which-one-is-better

Irfan, M. (2023, April 11). *Cotton fibers: Review of structure, properties, types and uses.* Cotton fibers: Review of structure, properties, types and uses. Cotton fibers: Review of structure, properties, types and uses.

Kalaoglu-Altan, O. I. (2022, January 30). *iScience*. Improving thermal conductivities of textile materials by nanohybrid approaches. https://pmc.ncbi.nlm.nih.gov/articles/PMC8867053/

Kempson, G. E., Clark, R. P., & Goff, M. R. (2007, May 31). The design, development and assessment of electrically heated gloves used for protecting cold extremities. *Ergonomics*, *31*(7), 1083-1091. https://doi.org/10.1080/00140138808966746

Kumar, N. (2004). *Comprehensive Physics XII*. Laxmi Publications. https://books.google.co.id/books?id=IryMtwHHngIC&pg=PA282#v=onepage&q&f=false

Ma, N., Lu, Y., Xu, F., & Dai, H. (2018, April 30). Development and performance assessment of electrically heated gloves with smart temperature control function. *International Journal of Occupational Safety and Ergonomics*, *26*(1), 46-54. https://doi.org/10.1080/10803548.2018.1457886

Meier, A. v. (2006). *Electric Power Systems: A Conceptual Introduction*. Wiley.

Pang, E., Pickering, S., Chan, A., & Wong, K. (2012, July 20). Use of recycled carbon fibre as a heating element. *Journal of Composite Materials*, *47*(16), 2039-2050. https://doi.org/10.1177/0021998312454033

Roofing Megastore. (n.d.). *Benefits of Sheep's Wool Insulation*. Benefits of Sheep's Wool Insulation. https://www.roofingmegastore.co.uk/blog/wool-insulation-benefits.html#:~:text=Sheep%20wool%20insulation%20boasts%20a,wool%20provides%20better%20insulative%20properties.

Ryan, C. (n.d.). *Monocrystalline vs Polycrystalline Solar Panels*. Oscilla enabling science. https://www.ossila.com/pages/monocrystalline-vs-polycrystalline-solar-panels#:~:text=Most%20polycrystalline%20solar%20panels%20have,perform%20better%20in%20warmer%20climates.

Short Guys Beta Works. (2023, January 9). *Are Battery-Heated Gloves Worth It for Backcountry Hiking, Camping, or Climbing?* YouTube. Retrieved January 18, 2025, from https://www.youtube.com/watch?v=8VdxlELXKk0

Wang, L. (2010, January 25). *Hand-Warmers*. C&EN. Retrieved January 16, 2025, from https://cen.acs.org/articles/88/i4/Hand-Warmers.html

Zhang, M. (2021, January 15). Building and Environment. *Numerical study of the convective heat transfer coefficient of the hand and the effect of wind*, *188*. https://www.sciencedirect.com/science/article/abs/pii/S0360132320308490#:~:text=Hands%20are%20highly%20vulnerable%20to,that%20for%20the%20whole%20body.

APPENDIX

Below are the documentations of the research project.